processes

MDPI

Article

Multi-Performance Optimization in Electrical Discharge Machining of Al_2O_3 Ceramics Using Taguchi Base AHP Weighted TOPSIS Method

Yue-Peng Zeng [1], Chiang-Lung Lin [1], Hong-Mei Dai [2], Yan-Cherng Lin [3] and Jung-Chou Hung [4,*]

1 Dongguan City College, Guangdong 523419, China; zengyp@ccdgut.edu.cn (Y.-P.Z.); chlulin@ccdgut.edu.cn (C.-L.L.)
2 College of Art, Zhongqiao Vocational and Technical University, Shanghai 201514, China; daihongmei@shzq.edu.cn
3 Department of Mechanical Engineering, Nan Kai University of Technology, Nantou 54243, Taiwan; ycline@nkut.edu.tw
4 Department of Mechanical Engineering, National Central University, Taoyuan 320, Taiwan
* Correspondence: hungjc@ncu.edu.tw

Abstract: The main application of electrical discharge machining in ceramic processing is limited to conductive ceramics. However, the most commonly used non-conductive potteries in modern industry, such as aluminum oxide (Al_2O_3), also reveal the limitations of choosing a suitable process. In this study, Taguchi based TOPSIS coupled with AHP weight method to optimize the machining parameters of EDM on Al_2O_3 leads to better multi-performance. The results showed that the technique is suitable for tackling multi-performance machining parameter optimization. The adhesive foil had a significant impact on material removal rate, electrode wear rate, and surface roughness, according to the findings. In addition, the response graph of relative closeness is used to determine the optimal combination levels of machining parameters. A confirmation test revealed a good agreement between predicted and experimental preference values at an optimum combination of the input parameters. The suggested experimental and statistical technique is a simple, practical, and reliable methodology for optimizing EDM process parameters on Al_2O_3 ceramics. This approach might be utilized to optimize and improve additional process parameters in the future.

Keywords: Taguchi method; EDM; TOPSIS method; AHP weight method; multi-performance

Citation: Zeng, Y.-P.; Lin, C.-L.; Dai, H.-M.; Lin, Y.-C.; Hung, J.-C. Multi-Performance Optimization in Electrical Discharge Machining of Al_2O_3 Ceramics Using Taguchi Base AHP Weighted TOPSIS Method. *Processes* **2021**, *9*, 1647. https://doi.org/10.3390/pr9091647

Academic Editor: Sung-Churl Choi

Received: 12 August 2021
Accepted: 9 September 2021
Published: 13 September 2021

1. Introduction

Electrical discharge machining (EDM) mainly produces high-temperature melting and vaporization of materials through discharge between electrodes, so the machinability of materials mostly depends on the thermal properties of materials, such as melting point, specific heat, thermal conductivity, etc.; however the mechanical properties of materials have little effect. It uses electric energy to convert into heat energy, which generates spark discharge in a certain small gap. The instant high temperature (6000 °C~12,000 °C) causes partial melting and evaporation on the surface of the workpiece, and then the flow of the working fluid and explosion of the pressure breaks away, and then achieves a processing method of material removal [1]. The principle of electrical discharge machining is to use resistors and capacitors to form a charging and discharging circuit, and to place conductive tool electrodes and workpieces in an insulating machining fluid. When electrical discharge machining is in progress, apply a voltage of tens to hundreds of volts between the two poles, and use the servo control system to control the tiny gap between the two poles, so that the tool electrode slowly approaches the workpiece. When the gap between the two poles reaches the maximum at a small distance from μm to tens of μm, the free ions in the machining fluid will gather due to the action of the electric field, and they will be arranged into an ion-intensive current path, which promotes the insulation breakdown of

the machining fluid between the two poles, forming a plasma channel; this is called the discharge phenomenon.

The above-mentioned discharge phenomenon occurs on a small local area. When it occurs, the high temperature generated causes the surrounding machining fluid to vaporize and expand due to the high temperature, and generate a great explosion pressure, which will wash away the molten material and achieve material removal. As the molten material that is washed away is cooled rapidly due to the low temperature of the surrounding processing fluid, forming processing chips are carried away by the flowing processing fluid. Other molten metals that have not been washed away are also cooled by the insulating liquid. It re-solidifies and remains on the surface of the workpiece to form a recast layer and discharge marks. At this point, the discharge column disappears, the pressure and temperature drop, and the original insulation state between the two poles is restored, and the first discharge process is completed, and the next pulse discharge is waited. Such a repeated discharge process can reach several times per second, ranging from hundreds up to hundreds of thousands of times, and continues to repeat until the required processing depth is completed.

EDM is suitable for the processing of super-hard conductive materials. Since most ceramic materials are electrical insulators, they have rarely been processed by EDM in the past. Ceramics come in three different types: conductive, semi-conductive, and non-conductive. In recent years, with the increasing application scope of non-conductive engineering ceramic materials, the processing performance of its surface is also highly requested. However, most of these materials are typical difficult-to-process materials, and it is generally difficult to meet the processing performance requirements using traditional contact processes. In recent years, both EDM and electrochemical discharge machining (ECDM) [2–4] have been studied to process non-conductive ceramic materials. However, the machining accuracy of ECDM still needs to be improved to meet the requirements of precision machining. In contrast, EDM still has advantages in machining accuracy and material removal rate. Since EDM is a non-contact thermo-physical process, it is necessary to re-understand the EDM process and explore its adaptability to non-conductive materials that has become another research hotspot in the field of EDM [5–9].

Apart from that, Mohri et al. [10] suggested the "Assisting Electrode Method" in the literature. In the Assisting Electrode technique, a conductive layer is applied to the surface of non-conductive ceramics. Electric sparks generate high temperatures, which cause dielectric oil hydrocarbon molecules and workpiece material molecules to break, allowing carbon to attach to particular parts of the ceramic. As carbon compounds are conductive, new discharges allow for the simultaneous machining of the deposited conductive layer and the workpiece material that was previously beneath the conductive layer. In the literature about EDM processing of non-conductive Al_2O_3 ceramic materials, Ferraris et al. [11] investigated the micro-EDM behavior of non-conductive ceramics made of zirconium dioxide and aluminum oxide, with a secondary conductive phase added within the insulating ceramic matrix. Due to the limitation associated with electrical discharge grinding and EDM, Liu et al. [12] devised electrical discharge milling to machine a bigger surface on a nonconductive aluminum oxide ceramic employing a thin copper sheet as an auxiliary layer. The electrical discharge machining mechanism of insulating noble sapphire crystals and three grades of high purity Al_2O_3 was also achieved by Fukuzawa et al. [13] using the helping electrode approach. Sung et al. [14] investigated the surface roughness and surface topography of GNP/Al_2O_3 ceramic composites using a continuous micro EDM milling method at various discharge energies. Muttamara et al. [15] compared the effect of the generation of conductive layers on alumina corresponding to EDM properties using copper, graphite and copper-impregnated graphite electrodes. It was found that the MRR value increased by 60% for the bipolar EDM-3. The surface roughness was improved to 25 μm at the anode of EDM-C3. Ji et al. [16] efficiently use high energy capacitors for EDM of insulating ceramics. The results show that high voltage, large capacitors, and high discharge energy can effectively process the insulating ceramic into EDM, and the single

discharge crater volume of the insulating ceramic can reach 17.63 mm^3. Liu et al. [17] present a new process for processing insulating ceramics using electric discharge (ED) milling cutters. The ED milling machine uses a water-based emulsion as the processing fluid, using a thin copper sheet as an auxiliary electrode, which is fed to the tool electrode along the surface of the workpiece. By using the flow rate of the machining fluid, the ED milling MRR is increased and the SR change is small. Liu et al. [18] uses a thin copper sheet fed to the tool electrode along the workpiece surface as an auxiliary electrode using an aqueous emulsion as the processing fluid. It can effectively treat large surface areas on insulating ceramics. The study results show that insulating Al_2O_3 ceramics are removed by a single pulse discharge under the influence of dissolution, evaporation, and delamination. The relevant ceramic EDM literature review is detailed in the review paper [19].

Dr. Genichi Taguchi developed the Taguchi Approach, which was a standardized Design of Experiment (DOE) method for identifying the optimum combination of variables under specified experimental circumstances [20]. The Taguchi approach [21] consists of three basic steps: orthogonal array selection, S/N ratio calculation, and analysis of variance (ANOVA). With a limited number of trials, an orthogonal array was designed to explore the whole parameter space [22,23]. Signal-to-noise ratio (S/N) identifies an optimal control factor setting that will make a process or product robust or tolerant of changes in noise factor. ANOVA was used to study the influence of process parameters on the machining process [24]. This method was best suited for single-performance optimization [25,26]. However, most industrial processes involve multi-response issues. As a result, a single-performance optimization issue may be converted into a multi-performance optimization problem using the Taguchi technique and the idea of Multi-Criteria Decision Making (MCDM). To choose the best processing conditions, the MCDM approach can be utilized.

The TOPSIS method was first proposed by Hwang and Yoon [27] that order preference method by similarity to ideal solution. The TOPSIS technique was an MCDM method for finding the best answer from a set of options when dealing with multiple criterion issues. The optimum solution has the smallest distance from the positive ideal solution and was the furthest away from the negative solution, according to the main principle of this approach. Therefore, TOPSIS based Taguchi optimization provides a useful approach to convert multi-performance simulation–optimization problem into the single-performance problem. In manufacturing, assessing multi-performance at the same time was an important issue. Balasubramaniyan, S. [28] used a combination of Taguchi and TOPSIS techniques to find the best process parameters for turning EN25 steel using coated carbide tools. Nahak, P. [29] applied TOPSIS and Taguchi method in turning austenitic stainless steel. TOPSIS and Taguchi method was to find the optimum machining parameters so as to minimize the surface roughness and tool cutting forces and maximize the material removal rate for the selected tool and work materials in the chosen domain of the experiment. Muqeem, M. [30] used the Taguchi-based entropy-weighted TOPSIS method to optimize the performance and emission parameters of diesel engines.

EDM process modeling and optimization in the EDM process is essential for multiple performance characteristic issues. Kasdekar, D. K. [31] proposed an entropy based TOPSIS, Simple Additive Weighting (SAW) methods to solve the multi-performance parameter optimization problem in EDM. Tripathy, S [32] using Taguchi method in combination with TOPSIS and grey relational analysis evaluated the effectiveness of optimizing multiple performance characteristics for powder mixed EDM of H-11 die steel using copper electrode. Vaddi, V. R. [33] focused on applying the Taguchi method and TOPSIS to optimize machining parameters in EDM of titanium alloys (Ti-6Al-4V), considering multiple performance issues. All of the findings showed that TOPSIS with Taguchi method was capable of addressing numerous objective issues involving EDM. A multi-performance problem was converted into a single equivalent objective problem using this technique. With the framework of a hierarchy of criteria, stakeholders, and results, and by drawing considerations for generating weights or priorities, this Analytic Hierarchy Process (AHP) approach [34] aids in the solution of complicated issues. It also synthesizes different factors into outcomes

that intuitively meet our expectations, combining the powers of sentiments and rationality focused on various topics. An AHP model's structure is that of an inverted tree. The objective of the decision-making problem is represented by a single purpose at the top of the tree. At this moment, the decision weight is 100 percent. A leaf point appears just below the objective, showing the qualitative and quantitative requirements. The goal weight should be distributed among the rating points according to the rating. In related literature, Nadda R. [35] used the hybrid AHP TOPSIS method to improve the surface roughness of cobalt-bonded tungsten carbide composites in EDM, maximize material removal rates, and minimize tool wear rates using optimal control parameter settings. We know that few studies have been reported on the application of the Taguchi method and TOPSIS method of EDM of non-conductive materials with multiple performance characteristics according to literature review.

As a result, the goal of this research is to determine the best process parameters for electrical discharge machining of non-conductive materials. Another important aspect of this study is that the TOPSIS method coupled with AHP method (which calculates relative weight of the performance variables) has been used to solve multi-performance optimization problem of EDM of non-conductive materials. The L18 orthogonal array of Taguchi method is used to conduct experiments. TOPSIS method is applied to determine the optimum conditions of process parameters to yield maximum MRR and minimum EWR simultaneously. The study results presented are significantly useful for researchers and professionals related to EDM of non-conductive materials with multiple performance characteristics.

2. Methodology and Experiments

2.1. Taguchi Method

The Taguchi method developed on the basis of orthogonal network (OA) experiments can greatly reduce the variance of the experiments and achieve the optimal settings of the control parameters. Therefore, the combination of the experimental design with the optimization of the control parameters to achieve the best results was obtained in the Taguchi method. Orthogonal arrays provide a good set of minimal tests, and signal-to-noise (S/N) ratios are log functions of the desired output, serving as objective functions for optimization, helping to analyze analysis data, and to predict optimal outcomes. There are 3 kinds of signal-to-noise ratios of common interest for optimization of static problems:

(I.) smaller-the-better:

$$\eta = -10 \log_{10}[\text{mean of sum of squares of measured data}] \quad (1)$$

This is usually the chosen S/N ratio for all undesirable characteristics like "defects, electrode wear rate, surface roughness", etc., for which the ideal value is zero.

(II.) larger-the-better:

$$\eta = -10 \log_{10}[\text{mean of sum squares of reciprocal of measured data}] \quad (2)$$

This case has been converted to a smaller case, the better by taking the inverse of the measured data and then taking the S/N ratio as in the smaller case, the better.

(III.) nominal-the-best:

$$\eta = -10 \log_{10}\left[\frac{\text{sqare of mean}}{\text{variance}}\right] \quad (3)$$

This situation occurs when a specified value is most desired, that is, no smaller or larger value is desired.

2.2. AHP Weighted TOPSIS Method

The main principle behind the TOPSIS approach is that the chosen alternative (suitable alternative) should be the closest to the positive ideal solution and the furthest away from

the negative ideal solution. The positive ideal solution maximizes the benefit criteria while minimizing the adverse criteria, whereas the negative ideal solution maximizes the adverse criteria while minimizing the benefit criteria. The following are the steps in the AHP weighted TOPSIS Method:

Step 1: This step involves the development of matrix format.

The rows of this matrix are assigned to an alternative and each column to an attribute. The decision matrix can be represented as follows:

$$D = \begin{matrix} A_1 \\ A_2 \\ \vdots \\ A_i \\ \vdots \\ A_m \end{matrix} \begin{bmatrix} x_{11} & x_{12} & \cdots & x_{1j} & x_{1n} \\ x_{21} & x_{22} & \cdots & x_{2j} & x_{2n} \\ \vdots & \vdots & \vdots & \vdots & \vdots \\ x_{i1} & x_{i2} & \cdots & x_{ij} & x_{in} \\ \vdots & \vdots & \vdots & \vdots & \vdots \\ x_{m1} & x_{m2} & \cdots & x_{mj} & x_{mn} \end{bmatrix} \quad (4)$$

where, A_i $(i = 1, 2, \cdots, m)$ represents the possible alternatives; X_j $(j = 1, 2, \cdots, n)$ represents the attributes related to alternative performance; and x_{ij} is the performance of A_i with respect to attribute X_j.

Step 2: Normalization of input data.

Obtain the normalized decision matrix r_{ij}. This can be represented as:
If the output value is of type maximizing, then the normalization equation is:

$$r_i(k) = \frac{x_i(k) - minx_i(k)}{maxx_i(k) - minx_i(k)} \quad (5)$$

If the output value is of type minimizing, then the normalization equation is:

$$r_i(k) = \frac{maxx_i(k) - x_i(k)}{maxx_i(k) - minx_i(k)} \quad (6)$$

where $r_i(k)$ represents normalized value of the kth element in ith sequence; $x_i(k)$ represents original sequence of x_{ij}, where i = 1, 2, 3 ... m and k = 1, 2, ... n; $maxx_i(k)$ represents highest value of $x_i(k)$; and $minx_i(k)$ is the lowest value of $x_i(k)$. Here, r_{ij} represents the normalized performance of A_i with respect to attribute X_j.

Step 3: Determination of weighted normalized decision matrix.

The weighted normalized decision matrix, $V = [v_{ij}]$ can be found as:

$$V = w_j r_{ij} \quad (7)$$

where, $\sum_j^n w_j = 1$.

The weight of the performance variables under different performances are calculated using the AHP method [36]. All judgments in the AHP technique are stored in a matrix of pairwise comparisons $A = [a_{ij}]_{mxn}$, where the dimension of matrix n is the number of parameters compared. The inverse comparison has been supplied to the member of the matrix aij, which represents a pairwise comparison of parameter i with parameter j (comparing parameter j with parameter i). As a result, the reciprocal value is:

$$a_{ij} = \frac{1}{a_{ji}} \quad (8)$$

In the case of group decision making where m is the number of decision makers, the individual judgments has been aggregated into one joint judgment a_{ij}^{group} applying the geometric mean method [37]:

$$a_{ij}^{group} = \sqrt[m]{\prod_{k=1}^{m} a_{ij}^{k}} \tag{9}$$

where a_{ij}^{k}, $k = 1, \ldots, m$ are the individual judgements of m decision makers.

To get the parameter weights from the matrix of pairwise comparisons A, the eigenvector technique may be used, which requires solving the equation:

$$Aw = \lambda_{max} w \tag{10}$$

where λ_{max} is the maximal eigenvalue of matrix A. For every matrix of pairwise comparisons A, the consistency ratio must also be calculated, which measures the level of inconsistency between pairwise comparisons:

$$CR = \frac{CI}{RI} \tag{11}$$

where $CI = \frac{\lambda_{max} - n}{n-1}$ is the consistency index, n is the size of matrix A and RI is the average consistency index. It can be assumed that if $CR \leq 0.10$, then the inconsistency level of matrix A is still acceptable.

Step 4: To determine the positive and negative ideal solutions.

The positive ideal solution A^+ indicates the most preferable alternative and the negative ideal, solution A^- indicate the least preferable alternative.

$$A^+ = \left\{v_1^+, v_2^+, \cdots, v_n^+\right\} = \left\{\left(\max_i v_{ij} | j \in J\right), \left(\min_i v_{ij} j \in J' | i = 1, 2, \cdots\cdots, m\right)\right\} \tag{12}$$

$$A^- = \left\{v_1^-, v_2^-, \cdots, v_n^-\right\} = \left\{\left(\min_i v_{ij} | j \in J\right), \left(\max_i v_{ij} j \in J' | i = 1, 2, \cdots\cdots, m\right)\right\} \tag{13}$$

where, $J = \{j = 1, 2, \cdots, n | j\}$: associated with the positive ideal solution attributes. $J' = \{j = 1, 2, \cdots, n | j\}$: associated with negative ideal solutions adverse attributes.

Step 5: Determine the distance measures.

The separation of each alternative from the ideal solution is given by n-dimensional Euclidean distance from the following equations:

$$S_i^+ = \sqrt{\sum_{j=1}^{n} \left(v_{ij} - v_j^+\right)^2}, i = 1, 2, \cdots\cdots, m \tag{14}$$

$$S_i^- = \sqrt{\sum_{j=1}^{n} \left(v_{ij} - v_j^-\right)^2}, i = 1, 2, \cdots\cdots, m \tag{15}$$

Step 6: Calculate the relative closeness to the ideal solution.

$$C_i^+ = \frac{S_i^-}{S_i^+ + S_i^-} \tag{16}$$

Step 7: Rank the preference order.

The alternative with the greater relative proximity is the best choice. In this study, the C_i^+ of each product called the multi-performance property index was optimized using the Taguchi method.

2.3. EDM Experiments

Experiments are conducted on EDM machine (Model CM 323C, CHMER Corp., Taichung City, Taiwan) choosing high purity of Al_2O_3 ceramics are adopted as workpiece materials and electrolytic copper as tool material. The schematic diagram of the experimental setup is shown in Figure 1. The properties of workpiece material and tool electrode material are shown in Tables 1 and 2, respectively. The dimensions of workpiece and electrode are 12 mm × 12 mm × 5 mm and 30 mm × 20 mm × 1.5 mm, respectively. Thus, a machined area of 1.5 mm × 5 mm would be formed on the machined surface of workpiece. The depth of 3 mm is the target of the process. Figure 2 shows the schematic diagram of EDM electrode and workpiece setting. The dielectric medium is a commercial kerosene dielectric fluid. The machined area is no flushing but the outside is. The pressure of flushing dielectric fluid is used as 0.1 kg/cm^2. The material properties of adhesive Cu and Al foils are showed in Table 3. The chemical composition of Cu and Al foils are showed in Table 4. The weight measurement in this experiment uses (Percisa XT 220A, Percisa Corp., Dietikon, Switzerland) precision electronic scale with an accuracy of 0.1 mg. Weigh before and after processing to calculate the weight loss and material removal rate. The stability of EDM progress is determined by inspecting the discharged waveforms. Thus, a fast and digital oscilloscope (Tektronix TDS 2014, Tektronix Corp., Beaverton, OR, USA) is employed in the experiments, which is in combination with a current probe (Chauvin Arnoux E3N, Chauvin Arnoux, Paris, France) and a passive voltage probe (Tektronix P2200, Tektronix Corp., Beaverton, OR, USA) to detect the waveforms of discharge current and voltage during the EDM process. The surface roughness is measured by the (Mitutoyo-surfest 4, Mitutoyo Corp., Kawasaki, Kanagawa, Japan) precision surface profile roughness meter, and the surface roughness value of the machined surface is measured in a random manner for 5 times, and the arithmetical mean height of a line (Ra) is calculated as the surface roughness evaluation standard. The cut-off length is used as 0.8 mm. The sample length is 4 mm.

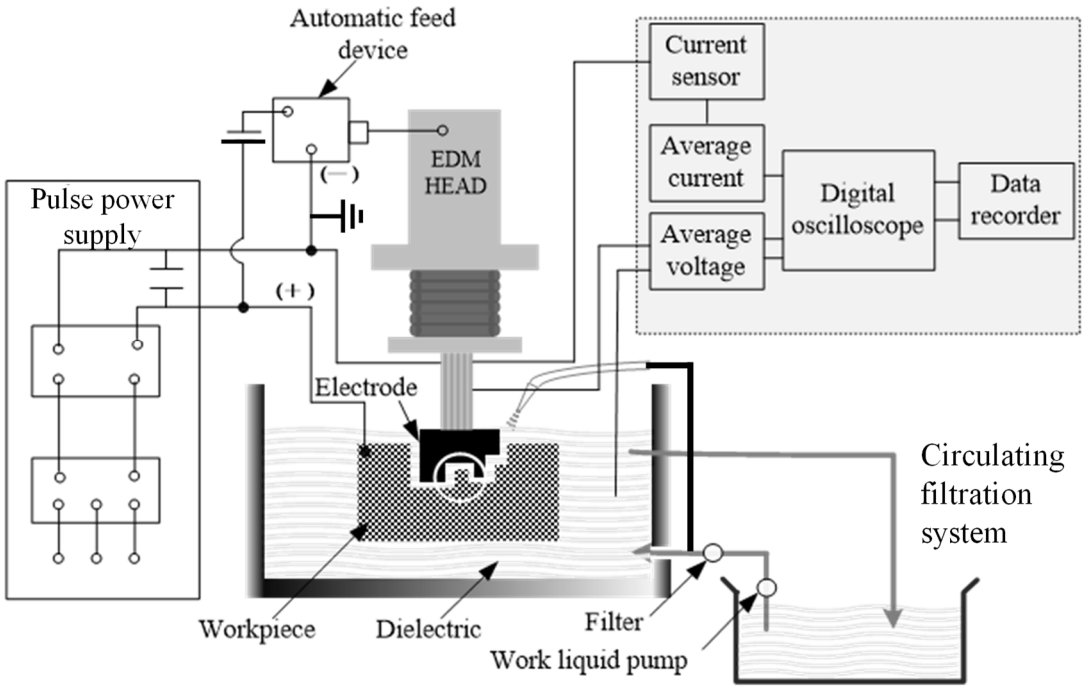

Figure 1. Schematic diagram of experimental system setup.

Table 1. Material properties of the Al_2O_3.

Properties	Descriptions
Specific gravity(g/cm^3)	3.96
Thermal conductivity (W/m K)	30–40
Electrical resistivity (Ω cm)	>10^{14}
Melting point (°C)	2050
Specific heat capacity (J/g °C)	0.75–0.85
Thermal expansion coefficient (1/°C)	5.5 × 10^{-6}

Table 2. Material properties of electrolytic copper electrode.

Properties	Descriptions
Specific gravity (g/cm^3)	8.94
Thermal conductivity (W/m K)	388
Electrical resistivity (Ω cm)	1.7 × 10^{-6}
Melting range (°C)	1065–1083
Specific heat capacity (J/g °C)	0.385
Thermal expansion coefficient (1/°C)	1.7 × 10^{-5}

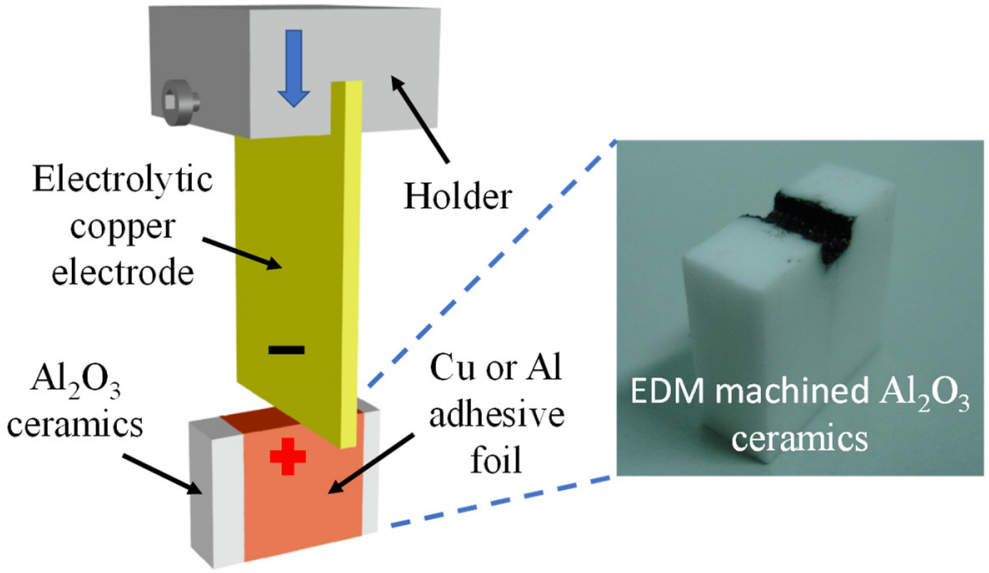

Figure 2. Schematic diagram of EDM electrode and workpiece setting.

Table 3. Material properties of adhesive Cu and Al foils.

Adhesive Foil Type	Cu	Al
Foil thickness (mm)	0.035	0.050
Acrylic adhesive thickness (mm)	0.025	0.030
Total thickness (mm)	0.06	0.08
Adhesion to steel (N/cm)	4.5	3.8
Tensile strength (N/cm)	40	22
Temperature resistance (°C)	−20 to 155	−20 to 110
Electrical resistance through adhesive (Ω cm)	0.003	0.020

Table 4. Chemical composition of Cu and Al foils.

Chemical Content	Cu Foils (%)	Al Foils (%)
Cu	Bal.	<0.050
Al	-	Bal.
Bi	<0.001	-
Sb	<0.002	-
As	<0.002	-
Fe	<0.005	<0.650
Pb	<0.005	-
S	<0.005	-
Si	-	<0.650
Mn	-	<0.050
Mg	-	<0.050
Zn	-	<0.100
Ti	-	<0.060
Others each	-	<0.030

In this study, Taguchi parameter design is adopted to optimize the EDM parameter settings for the Al_2O_3 ceramics. The control factors including five factors with three levels and one factor with two levels are considered that refers to [8]. Table 5 shows the values of the machining parameters and their levels. In the processing of non-conductive ceramics, the purpose of the auxiliary electrode is to generate electric discharge in the early stage of processing, and to promote the production of carbon in the kerosene dielectric fluid to maintain the continuous electric discharge processing. Therefore, generally speaking, only a very thin conductive metal layer is sufficient. In this study, the thickness difference between the two is only 0.015 mm. The depth of 3 mm is the target of the process. The study ignores the effect of the difference in the thickness of the metal adhesive foil. Auxiliary current with high voltage means each discharge will use an auxiliary current accompanied by a high voltage to break through the state of insulation between electrodes. Electrode jumping-up time refers to the interval between the end of this jump and the next one. The workpiece material used in this study is a non-conductive ceramic material, the discharge relies on the carbon existing in the machining gap to perform continuous EDM. The electrode jump time will affect the carbon concentration in the gap and affect the discharge. characteristic. Therefore, this parameter is specially added to the discussion. The range of jumping-up time can be set from 0.1 to 10 s in this EDM machine. When the setting time is longer, the processing volume during the process is larger, which will easily cause poor slag discharge. The relative closeness value refers to the relative closeness of the experimental value to the target value. Taguchi's experimental design is an experimental method that uses orthogonal tables to select experimental conditions and schedule experiments. Orthogonal Array is the basic tool for orthogonal experimental design. A kind of normalized table constructed on the basis of the orthogonal Latin side of the combination mathematical theory. Its symbol is Ln (j^i) where: L—orthogonal table code n—number of rows of orthogonal table, that is, the number of experiments, j—digital in the orthogonal table, that is, the number of bits of factors, I—the number of columns of orthogonal tables, i.e., the number of experimental factors, is an example of a mixed-bit orthogonal table L18 (21×37) structure. The Taguchi experimental design used in this paper is based on following: (1) The number of experiments can be reduced from 2×3^5 to 18. (2) When an orthogonal table is used, a full grid cannot be scheduled so that G and H space arrangement is considered as an experimental test error. Therefore, a L18 orthogonal array is selected for this study. Table 6 shows the experimental layout using a L18 orthogonal array.

Table 5. Machining parameters and their levels.

Code	Parameters	Unit	Level 1	Level 2	Level 3
A	Adhesive foil (Type)		Cu	Al	-
B	Peak current (I_p)	A	2	3	4
C	Auxiliary current with high voltage (I_H)	A	0.4	0.98	1.2
D	Pulse duration (τ_p)	µs	50	100	200
E	Electrode jumping-up time (EJT)	sec	2	3	4
F	Servo reference voltage (S_v)	V	40	55	70

Table 6. Experimental layout in a L_{18} ($2^1 \times 3^7$) orthogonal array.

No.	Parameter Level							
	A	**B**	**C**	**D**	**E**	**F**	**G**	**H**
	Type	**I_p**	**I_H**	**τ_p**	**EJT**	**Sv**	**E**	**E**
1	1	1	1	1	1	1	1	1
2	1	1	2	2	2	2	2	2
3	1	1	3	3	3	3	3	3
4	1	2	1	1	2	2	3	3
5	1	2	2	2	3	3	1	1
6	1	2	3	3	1	1	2	2
7	1	3	1	2	1	3	2	3
8	1	3	2	3	2	1	3	1
9	1	3	3	1	3	2	1	2
10	2	1	1	3	3	2	2	1
11	2	1	2	1	1	3	3	2
12	2	1	3	2	2	1	1	3
13	2	2	1	2	3	1	3	2
14	2	2	2	3	1	2	1	3
15	2	2	3	1	2	3	2	1
16	2	3	1	3	2	3	1	2
17	2	3	2	1	3	1	2	3
18	2	3	3	2	1	2	3	1

Material removal rate (*MRR*), electrode wear rate (*EWR*), and surface roughness (SR) are considered as performance characteristics. The performance parameters like the material removal rate and electrode wear rate are calculated using the following expressions:

$$MRR(mm^3/min) = \frac{\Delta w}{\rho_w \times t} \tag{17}$$

$$EWR(g/min) = \frac{\Delta T}{\rho_t \times t} \tag{18}$$

where Δw is the weight difference of workpiece before and after machining (g), ρ_w is density of workpiece material (g/mm^3), ΔT is the weight difference of electrode before and after machining (g), and ρ_t is density of electrode material (g/mm^3). At last, surface roughness values are measured on a surface profile meter. The output performance characteristics (material removal rate, tool wear rate and surface roughness) have been evaluated through the experiments presented in Table 7.

Table 7. Experimental result for machining performance.

No.	Material Removal Rate, MRR (mm^3/min)	Electrode Wear Rate, EWR (g/min)	Surface Roughness, SR (μm)
1	0.0121	0.0160	11.60
2	0.0121	0.0194	15.40
3	0.0467	0.0205	15.60
4	0.0233	0.0142	14.40
5	0.0551	0.0213	15.40
6	0.0738	0.0164	16.66
7	0.0654	0.0160	16.30
8	0.1008	0.0145	17.00
9	0.0719	0.0250	14.42
10	0.0906	0.0119	14.70
11	0.0047	0.0019	11.20
12	0.0308	0.0056	11.60
13	0.0177	0.0037	17.16
14	0.1354	0.0116	16.18
15	0.0280	0.0048	12.60
16	0.0598	0.0030	24.94
17	0.0224	0.0056	13.56
18	0.1615	0.0119	20.18

3. Results and Discussion

3.1. Determination of S/N Ratios

In this study, two observed values of EWR, SR and MRR are explored. The experimentally observed EWR, SR values are the smaller-the-better quality characteristics and MRR values are the larger-the-better quality characteristics. Therefore, the optimal observed EWR, SR values are minimum value, and the optimal MRR is the maximum value. Based on the Taguchi parameter design, the S/N ratio calculation is chosen as the smaller-the-better and larger-the-better as given in Equations (1) and (2). The S/N ratio of EWR, SR and MRR are shown on Table 8.

Table 8. S/N ratio (η) of EWR, SR, and MRR.

No.	MRR	EWR	SR
1	−38.317	35.900	−21.289
2	−38.317	34.249	−23.750
3	−26.616	33.762	−23.862
4	−32.637	36.974	−23.167
5	−25.179	33.452	−23.750
6	−22.643	35.700	−24.433
7	−23.694	35.900	−24.244
8	−19.927	36.748	−24.609
9	−22.866	32.048	−23.179
10	−20.860	38.466	−23.346
11	−46.616	54.590	−20.984
12	−30.226	45.047	−21.289
13	−35.021	48.569	−24.690
14	0.1354	0.0116	16.18
15	0.0280	0.0048	12.60
16	0.0598	0.0030	24.94
17	0.0224	0.0056	13.56
18	0.1615	0.0119	20.18

3.2. Normalization of Input Data

Equations (5) and (6) are used to normalize the computed S/N ratio of specified targets (6). If the MRR value is of the maximizing kind, the normalization equation is as

follows: (5). If the EWR, SR value is of the minimization type, the normalization equation is as follows: (6). Table 9 shows the normalized choice matrix.

Table 9. Normalized decision matrix.

No.	MRR	EWR	SR
1	0.270	0.829	0.044
2	0.270	0.902	0.398
3	0.650	0.924	0.414
4	0.454	0.781	0.314
5	0.696	0.938	0.398
6	0.779	0.838	0.496
7	0.745	0.829	0.469
8	0.867	0.791	0.521
9	0.772	1.000	0.316
10	0.837	0.715	0.340
11	0.000	0.000	0.000
12	0.532	0.423	0.044
13	0.377	0.267	0.533
14	0.950	0.703	0.460
15	0.506	0.368	0.147
16	0.719	0.181	1.000

3.3. Determination of Weighted Normalized Decision Matrix

In this study, three experts set up the pairwise comparison matrix of performance characterizes first, and then the group integration judgment matrix of performance characterizes is solved by the geometric average method of column vectors. The results are shown in Table 10.

Table 10. The judgement matrix of group integration for performance characteristics.

	Material Removal Rate	Electrode Wear Rate	Surface Roughness
Material removal rate	1.000	1.000	1.587
Electrode wear rate	1.000	1.000	0.794
Surface roughness	0.630	1.260	1.000

Using the AHP methodology obtains the weights of the performance characteristics (material removal rate, electrode wear rate and surface roughness) are calculated as 0.386, 0.307, and 0.307, respectively. The value of λ_{max} is 3.054 and consistency ratio (CR) is 0.046, which is much less than the allowed CR value of 0.1. Thus, there is good consistency in the judgment of relative importance matrix. The performance characteristic and weighted (normalized) decision matrix has been shown in Table 11.

Table 11. Weighted normalized decision matrix.

No.	MRR	EWR	SR
1	0.104	0.255	0.013
2	0.104	0.277	0.122
3	0.251	0.284	0.127
4	0.175	0.240	0.096
5	0.269	0.288	0.122
6	0.301	0.257	0.152

Table 11. *Cont.*

No.	MRR	EWR	SR
7	0.287	0.255	0.144
8	0.335	0.243	0.160
9	0.298	0.307	0.097
10	0.323	0.220	0.104
11	0.000	0.000	0.000
12	0.206	0.130	0.013
13	0.145	0.082	0.164
14	0.367	0.216	0.141
15	0.195	0.113	0.045
16	0.278	0.056	0.307
17	0.171	0.130	0.073
18	0.386	0.220	0.226

3.4. Determination of Relative Closeness (C_i) to Positive Ideal Solution

Determination of positive ideal solution (A^+) and negative ideal solution (A^-). A^+ and A^- are determined using Equations (12) and (13).

$$A^+_{MRR} = 0.386,\ A^+_{EWR} = 0.000,\ A^+_{SR} = 0.000$$
$$A^-_{MRR} = 0.000,\ A^-_{EWR} = 0.307,\ A^-_{SR} = 0.307$$

Now the separation distance is measured from both positive ideal solution and negative ideal solution using Equations (14) and (15) and then the relative closeness index is calculated using Equation (16) and tabulated in Table 12.

Table 12. Separation measure of positive ideal solution, negative ideal solution, and relative closeness value.

No.	S_i^+	S_i^-	C_i
1	0.380	0.316	0.454
2	0.414	0.214	0.341
3	0.339	0.310	0.477
4	0.334	0.282	0.458
5	0.334	0.327	0.495
6	0.311	0.342	0.524
7	0.309	0.335	0.520
8	0.295	0.371	0.557
9	0.334	0.364	0.522
10	0.251	0.391	0.609
11	0.386	0.434	0.529
12	0.223	0.400	0.642
13	0.302	0.304	0.501
14	0.259	0.413	0.615
15	0.226	0.380	0.627
16	0.330	0.375	0.531
17	0.262	0.339	0.564
18	0.315	0.404	0.562

3.5. Determination of Optimum Parameters Levels

The Taguchi base AHP weighted TOPSIS technique analyzes experimental findings based on relative proximity. Table 12 shows the estimated relative closeness values for the higher degree of relative closeness values utilized to discover combinations of machining parameters. Based on the performance table for the relative closeness value (Table 13) and the main effects plot (Figure 3), the optimum machining parameters are adhesive foil of Al (A_2), peak current of 4 A (B_3), auxiliary current with high voltage of 1.2 A (C_3), pulse duration of 200 µs (D_3), electrode jumping-up time of 2 s (E_1), and servo reference voltage

of 40 V (F_1). As mentioned above, when the peak current, auxiliary current with high voltage, and pulse duration were set at high levels, a considerable amount of workpiece material was removed because to the evident material removal mechanisms that were created in the machining zone when a substantial amount of discharge energy was supplied into the machining zone in a single pulse. In the non-insulating ceramic electric discharge machining process, the metal adhesive foil plays the role of the initial arc ignition discharge. During the electric discharge machining process, the commercial kerosene dielectric fluid cause dielectric oil hydrocarbon molecules and workpiece material molecules to resolve due to the high temperature discharge arc, allowing carbon to attach to particular parts of the ceramic. According to the literature, the energy density required for Cu material unit to be EDM is 3.2×10^7 (W/cm^2), and the energy density required for Al material unit to be EDM is 1.5×10^7 (W/cm^2) [38]. Therefore, the required processing thickness (Cu is 0.035 mm; Al is 0.050 mm) is calculated with the energy density required for electrical discharge processing per unit of material; the processing time of Cu foil and Al foil is about 3:2 under the same electrical discharge conditions. In this experiment, due to the relatively thick thickness of the Al adhesive foil, the influence on the initial processing is greater than the influence time of the Cu adhesive foil. At this time, the insulating liquid includes carbon and metal debris, and when the metal adhesive foil is consumed, the deeper the processing depth, the debris influence of the metal foil will gradually decrease. The middle and late stages are mainly the process of the carbon decomposed by the insulating oil. The electric discharge circuit keeps the machining going.

Table 13. Performance table for the relative closeness value.

Symbol	Parameters	Level 1	Level 2	Level 3	Max-Min
A	Adhesive foil	0.483	0.576	-	0.093
B	Peak current	0.509	0.537	0.543	0.028
C	Auxiliary current with high voltage	0.512	0.517	0.559	0.005
D	Pulse duration	0.526	0.510	0.552	0.016
E	Electrode jumping-up time	0.534	0.526	0.528	0.008
F	Servo reference voltage	0.540	0.518	0.530	0.022

noindentTotal mean relative closeness value = 0.529.

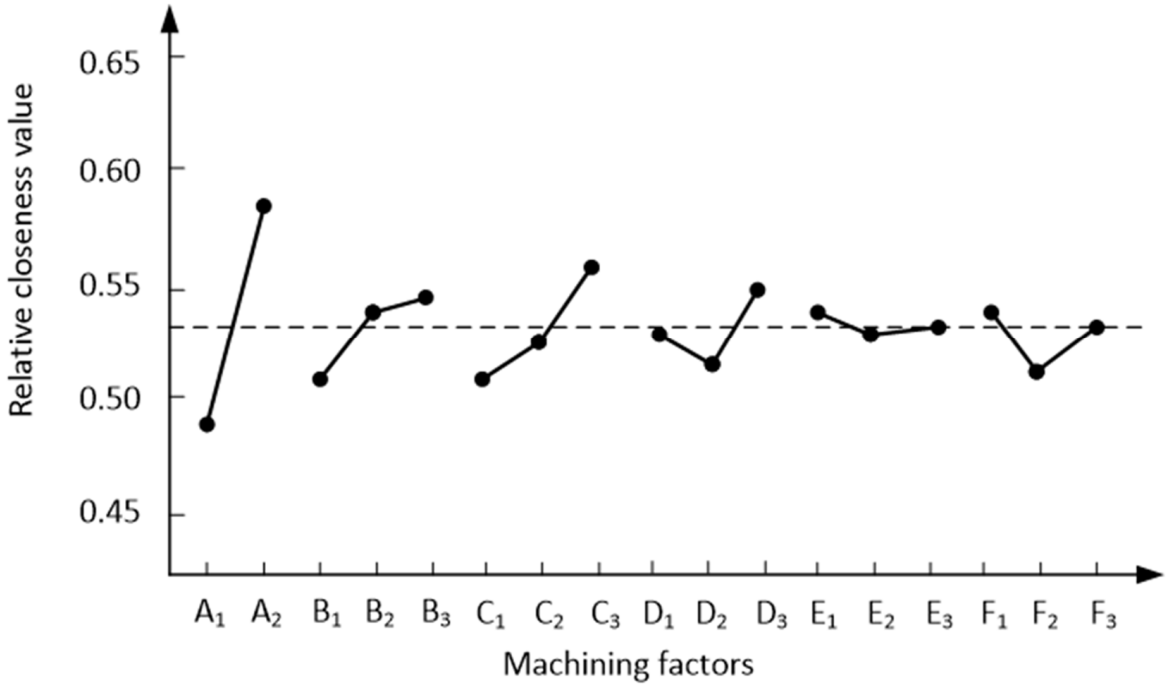

Figure 3. The relative closeness value graph.

3.6. Calculation of ANOVA

ANOVA is used to examine the experimental data and determine which process factors have a significant influence. ANOVA determines the significant effects for regulating performance, parameter contribution in terms of percentage, and error variance in the process. The most important process parameter is adhesive foil. The ANOVA findings are shown in Table 14.

Table 14. Results of the analysis of variance.

Symbol	Parameters	Degree of Freedom	Sum of Squares	Mean Squares	F	Contribution (%)
A	Adhesive foil	1	0.039	0.039	7.148	42.901
B	Peak current	2	0.004	0.002	0.364	4.367
C	Auxiliary current with high voltage	2	0.008	0.004	0.733	8.804
D	Pulse duration	2	0.005	0.003	0.500	6.001
E	Electrode jumping-up time	2	0.000	0.000	0.019	0.226
F	Servo reference voltage	2	0.002	0.001	0.141	1.687
Error		6	0.032	0.005		36.013
Total		17	0.090			100

3.7. Confirming Results

To assess performance characteristics for EDM of Al_2O_3 ceramics, confirmation tests for the optimum parameters with their levels are done. Table 15 shows the initial process parameter ($A_1B_2C_2D_2E_2F_2$) set of material removal rate, electrode wear rate, surface roughness, and C_i values. Additionally, it shows the comparison of the experimental results for the optimal conditions ($A_2B_3C_3D_3E_1F_1$) with predicted results for optimal ($A_2B_3C_3D_3E_1F_1$) EDM parameters. The predicted values are obtained by:

$$\textit{Predicted Response} = \textit{Average of } A_2 + \textit{Average of } B_3 + \textit{Average of } C_3 + \textit{Average of } D_3 + \textit{Average of } E_1 + \textit{Average of } F_1 - 5 \times \textit{Mean of response} \quad (19)$$

Table 15. Results of machining performance using the initial and optimal machining factors.

	Initial Parameters	Optimal Parameters		%Error
		Prediction	Experiment	
Levels	$A_1B_2C_2D_2E_2F_2$	$A_2B_3C_3D_3E_1F_1$	$A_2B_3C_3D_3E_1F_1$	
Material removal rate (mm^3/min)	0.055	0.132	0.126	4.762
Electrode wear rate (g/min)	0.012	0.007	0.0067	4.478
Surface roughness (μm)	15.40	18.69	16.25	15.015
Relative closeness value	0.548	0.619	0.655	4.622

Following the discovery of the anticipated values, confirmation experiments are carried out using an optimal parametric setup. Further, projected values are compared to experimental data, and deviation is computed as a percentage of error related to each performance feature, using the equation below.

$$\%error = \frac{|experimental\ valve - predicted\ valve|}{predicted\ valve} \times 100 \quad (20)$$

The performance values obtained from the conformation experiment are MRR of 0.126 mm^3/min, EWR of 0.0067 g/min, and the surface roughness of 16.25 μm at adhesive foil of Al, peak current of 4 A, auxiliary current with high voltage of 1.2 A, pulse duration of 200 μs, electrode jumping-up time of 2 sec, and servo reference voltage of 40 V. As the results indicate that the percent error correlated with MRR and EWR for the optimal combination levels of machining parameters are 4.762 and 4.478 higher than those obtained at the initial experimental conditions $A_1B_2C_2D_2E_2F_2$ but the percent error of surface roughness is 15.015.

Figure 4 showed two SEM images of EDM machined area of (a) Al adhesive foil and (b) Cu adhesive foil. It can be seen from the figure that the surface roughness obtained by using Al adhesive foil is better than using Cu adhesive foil. The comparison again shows the good agreement between the predicted and the experimental values shown in Table 15. The percent error of relative closeness value could be achieved as 4.622.

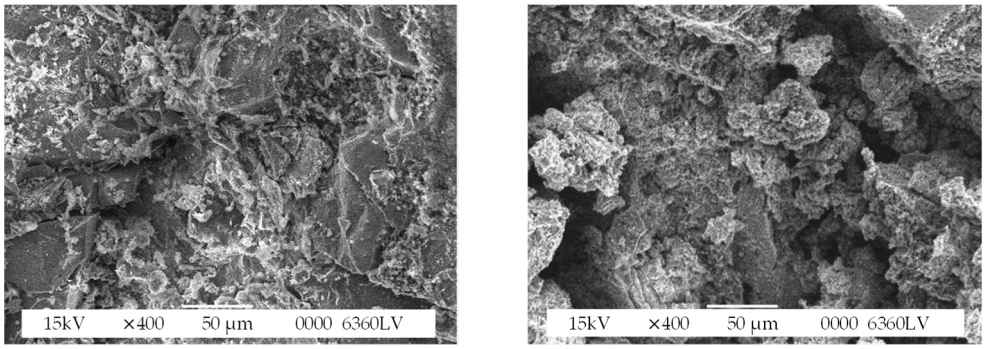

(**a**) (**b**)

Figure 4. SEM images of EDM machined area of (**a**) Al adhesive foil and (**b**) Cu adhesive foil. (Peak current of 4 A, auxiliary current with high voltage of 1.2 A, pulse duration of 200 µs, electrode jumping-up time of 2 s, and servo reference voltage of 40 V.)

In reference [9], the authors found an MRR of 0.078 mm^3/min and SR of 2.589 µm at adhesive copper (Cu) foil, 1.1 A peak current, 6 µs pulse-on time, and 14 V gap voltage in sinking EDM. In a method similar to this research, it was found that the use of adhesive copper (Cu), a smaller peak current, and the gap voltage achieved better SR. The authors of [12] found an MRR of 60.6 mm^3/min and SR of 11 µm at thin red copper sheet, rotational speed of 1000 r/min, pulse duration of 500 µs, pulse interval of 350 µs, peak current of 25 A, and tool electrode as positive polarity in ED milling. The MRR was quite outstanding, but its processing method was different from this method. Both studies used a single quality method. In this paper, the multiple quality methods are used, so maximum material removal rate of 0.126 mm^3/min, minimum electrode wear rate of 0.0067 g/min, and general SR of 16.25 µm could be obtained at optimum machining parameters.

4. Conclusions

This study demonstrates the application of the Taguchi base AHP weighted TOPSIS method, which helps process engineers in selecting the most optimal process parameter from a large number of conflicting factors for performing EDM on Al_2O_3 ceramics. TOPSIS based multi-performance optimization strategy was used. AHP method was used to find the weight of the response variables under different performance. Experiments were performed as per Taguchi's standard L18 orthogonal array. Results obtained from the relative closeness to the ideal solutions were used to rank the preference order in the selection of optimum process parameter. It was noticed that the best choice of optimum process parameters was adhesive foil of Al, a peak current of 4 A, an auxiliary current with high voltage of 1.2 A, a pulse duration of 200 µs, an electrode jumping-up time of 2 s, and servo reference voltage of 40 V, which gives a maximum material removal rate of 0.126 mm^3/min, a minimum electrode wear rate of 0.0067 g/min, and a surface roughness of 16.25 µm. The confirmation test showed good agreement between the predicted and experimental preference values at the optimal combination of the input parameters. The percent error of relative closeness value could be achieved as 4.622. The suggested experimental and statistical technique is a simple, practical, and reliable methodology for optimizing EDM process parameters on Al_2O_3 ceramics. This approach might be utilized to optimize and improve additional process parameters in the future. This approach can also be used to investigate other machining methods.

Author Contributions: Methodology, C.-L.L. and Y.-C.L.; validation, Y.-C.L.; formal analysis, C.-L.L. and Y.-C.L.; investigation, Y.-P.Z., C.-L.L., H.-M.D., Y.-C.L. and J.-C.H.; resources, Y.-P.Z., C.-L.L. and Y.-C.L.; data curation, C.-L.L. and Y.-C.L.; writing—original draft preparation, Y.-P.Z., C.-L.L., H.-M.D., Y.-C.L. and J.-C.H.; writing—review and editing, C.-L.L. and J.-C.H.; visualization, J.-C.H.; supervision, Y.-P.Z., H.-M.D. and J.-C.H.; project administration, C.-L.L. and J.-C.H.; funding acquisition, Y.-P.Z. and Y.-C.L. All authors have read and agreed to the published version of the manuscript.

Funding: This research received no external funding.

Institutional Review Board Statement: Not applicable.

Informed Consent Statement: Informed consent was obtained from all subjects involved in the study.

Data Availability Statement: The data and materials are available.

Conflicts of Interest: The authors declare no conflict of interest.

References

1. Emmanouil, L.P.; Panagiotis, K.O.; Beata, L.-M.; Angelos, P.M. A study on Electrical Discharge Machining of Titanium Grade2 with experimental and theoretical analysis. *Sci. Rep.* **2021**, *11*, 8971.
2. Chak, S.K.; Rao, P.V. The drilling of Al2O3 using a pulsed DC supply with a rotary abrasive electrode by the electrochemical discharge process Int. *J. Adv. Manuf. Technol.* **2008**, *39*, 633–641. [CrossRef]
3. Jain, V.K.; Chak, S.K. Electrochemical Spark Trepanning of Alumina and Quartz. *Mach. Sci. Technol.* **2000**, *4*, 277–290. [CrossRef]
4. Chak, S.K.; Rao, P.V. Trepanning of Al2O3 by electro-chemical discharge machining (ECDM) process using abrasive electrode with pulsed DC supply. *Int. J. Mach. Tools Manuf.* **2007**, *47*, 2061–2070. [CrossRef]
5. Lin, Y.C.; Chen, Y.F.; Lin, C.T.; Tzeng, H.J. Electrical Discharge Machining (EDM) Characteristics Associated with Electrical Discharge Energy on Machining of Cemented Tungsten Carbide. *Mater. Manuf. Process* **2008**, *23*, 391–399. [CrossRef]
6. Cheng, Y.M.; Eubank, P.T.; Gadalla, A.M. Electrical Discharge Machining of ZrB2-Based Ceramics. *Mater. Manuf. Process* **1996**, *11*, 565–574. [CrossRef]
7. Trueman, C.S.; Huddleston, J. Material removal by spalling during EDM of ceramics. *J. Eur. Ceram. Soc.* **2000**, *20*, 1629–1635. [CrossRef]
8. Lin, Y.C.; Hung, J.C.; Chow, H.M.; Wang, A.C. Optimization of EDM parameters for ZrO2 and Al2O3 ceramics using Taguchi method. *J. Ceram. Process. Res.* **2015**, *16*, 249–257.
9. Ali, M.Y.; Moudood, M.A.; Maleque, M.A.; Hazza, M.; Adesta, E.Y.T. Electro-discharge machining of alumina: Investigation of material removal rate and surface roughness. *J. Mech. Eng. Sci.* **2017**, *11*, 3015–3026. [CrossRef]
10. Mohri, N.; Fukuzawa, Y.; Tani, T.; Saito, N.; Furutani, K. Assisting electrode method for machining insulating ceramics. *CIRP Ann. Manuf. Technol.* **1996**, *45*, 201–204. [CrossRef]
11. Ferraris, E.; Reynaerts, D.; Lauwers, B. Micro-edm process investigation and comparison performance of Al3O2 and ZrO2 based ceramic composites. *CIRP Ann. Manuf. Technol.* **2011**, *60*, 235–238. [CrossRef]
12. Liu, Y.; Li, X.; Ji, R.; Yu, L.; Zhang, H.; Li, Q. Effect of technological parameter on the process performance for electric discharge milling of insulating Al2O3 ceramic. *J. Mater. Process. Technol.* **2008**, *208*, 245–250. [CrossRef]
13. Fukuzawa, Y.; Mohri, N.; Tanic, T.; Muttamara, A. Electrical discharge machining properties of noble crystals J. *Mater. Process. Technol.* **2004**, *149*, 393–397. [CrossRef]
14. Sung, J.W.; Kim, K.H.; Kang, M.C. Effects of Graphene Nanoplatelet Contents on Material and Machining Properties of GNP-Dispersed Al2O3 Ceramics for Micro-Electric Discharge Machining Int. *J. Precis. Eng. Manuf. Green Technol.* **2016**, *3*, 247–252. [CrossRef]
15. Muttamara, A.; Fukuzawa, Y.; Mohri, N.; Tani, T. Effect of electrode material on electrical discharge machining of alumina. *J. Mater. Process. Technol.* **2009**, *209*, 2545–2552. [CrossRef]
16. Ji, R.; Liu, Y.; Zhang, Y.; Zhang, H.; Li, X.; Dong, X. An experimental research on single discharge machining of insulating ceramics efficiently with high energy capacitor. *Sci. China Technol. Sci.* **2011**, *54*, 1537–1545. [CrossRef]
17. Liu, Y.; Ji, R.; Li, X.; Yu, L.; Zhang, H.; Li, Q. Effect of machining fluid on the process performance of electric discharge milling of insulating Al2O3 ceramic. *Int. J. Mach. Tools Manuf.* **2008**, *48*, 1030–1035. [CrossRef]
18. Liu, Y.; Yu, L.; Xu, Y.; Ji, R.; Li, Q. Numerical simulation of single pulse discharge machining insulating Al2O3 ceramic. *Proc. Inst. Mech. Eng. Part B J. Eng. Manuf.* **2009**, *223*, 55–62. [CrossRef]
19. Bilal, A.; Jahan, M.P.; Talamona, D.; Perveen, A. Electro-Discharge Machining of Ceramics: A Review. *Micromachines* **2019**, *10*, 10. [CrossRef]
20. Taguchi, G.K.S.; Konishi, S. *Taguchi Methods Orthogonal Arrays and Linear Graphs: Tools for Quality Engineering*; American Supplier Institute: Dearborn, MI, USA, 1987.
21. Karna, S.K.; Sahai, R. An Overview on Taguchi Method. *Int. J. Eng. Math. Sci.* **2012**, *1*, 1–7.
22. Hanif, M.I.; Aamir, M.; Ahmed, N.; Maqsood, S.; Muhammad, R.; Akhtar, R.; Hussain, I. Optimization of facing process by indigenously developed force dynamometer. *Int. J. Adv. Manuf. Technol.* **2019**, *100*, 1893–1905. [CrossRef]

23. Yang, W.P.; Tarng, Y. Design optimization of cutting parameters for turning operations based on the Taguchi method. *J. Mater. Process. Technol.* **1998**, *84*, 122–129. [CrossRef]
24. Ribeiro, J.E.; César, M.B.; Lopes, H. Optimization of machining parameters to improve the surface quality. *Proced. Struct. Integr.* **2017**, *5*, 355–362. [CrossRef]
25. Lee, D.H.; Park, J.S.; Ryu, M.R.; Park, J.H. Development of a highly efficient low emission diesel engine-powered co-Generation system and its optimization using Taguchi method. *Appl. Therm. Eng.* **2013**, *50*, 491–495. [CrossRef]
26. Wu, H.W.; Wu, Z.Y. Using Taguchi method on combustion performance of a diesel engine with diesel/Biodiesel blend and port-inducting H2. *Appl. Energy* **2013**, *104*, 362–370. [CrossRef]
27. Hwang, C.L.; Yoon, K. *Multiple Attribute Decision Making Methods and Applications*; A State-of-the-Art Survey; Springer: Berlin/Heidelberg, Germany, 1981.
28. Balasubramaniyan, S.; Selvaraj, T. Application of integrated Taguchi and TOPSIS method for optimization of process parameters for dimensional accuracy in turning of EN25 steel. *J. Chin. Inst. Eng.* **2017**, *40*, 267–274. [CrossRef]
29. Nahak, P.; Dubey, M. Optimization in Turning Austenitic Stainless Steel using TOPSIS and Taguchi Method. *Int. J. Eng. Manag. Res.* **2016**, *6*, 428–434.
30. Muqeem, M.; Sherwani, A.F.; Ahmad, M.; Khan, Z.A. Application of the Taguchi based entropy weighted TOPSIS method for optimisation of diesel engine performance and emission parameters. *Int. J. Heavy Veh. Syst.* **2019**, *26*, 69–94. [CrossRef]
31. Kasdekar, D.K.; Parashar, V. MADM Approach for Optimization of Multiple Responses in EDM of En-353 Steel. *Int. J. Adv. Sci. Technol.* **2015**, *83*, 59–70. [CrossRef]
32. Tripathy, S.; Tripathy, D.K. Multi-attribute optimization of machining process parameters in powder mixed electro-discharge machining using TOPSIS and grey relational analysis. *Eng. Sci. Technol. Int. J.* **2016**, *19*, 62–70. [CrossRef]
33. Vaddi, V.R.; Ch, S.R.; Bushaboina, S.K.; Banka, H. Application of TOPSIS with Taguchi Method for Multi-Attribute Optimization of Machining Parameters in EDM. *SAE Tech. Pap. Ser.* **2018**, 2018-28-0033. [CrossRef]
34. Widianta, M.M.D.; Rizaldi, T.; Setyohadi, D.P.S.; Riskiawan, H.Y. Comparison of Multi-Criteria Decision Support Methods (AHP, TOPSIS, SAW & PROMENTHEE) for Employee Placement. *J. Phys. Conf. Ser.* **2018**, *953*, 012116.
35. Nadda, R.; Kumar, R.; Singh, T.; Chauhan, R.; Patnaik, A.; Gangil, B. Experimental investigation and optimization of cobalt bonded tungsten carbide composite by hybrid AHP-TOPSIS approach. *Alex. Eng. J.* **2018**, *57*, 3419–3428. [CrossRef]
36. Saaty, T.L. *The Analytic Hierarchy Process*; McGraw-Hill: New York, NY, USA, 1980.
37. Saaty, T.L.; Özdemir, M.S. How Many Judges Should There Be in a Group? *Ann. Data Sci.* **2015**, *1*, 359–368. [CrossRef]
38. Saito, C. *Illustrated EDM Mechanism and 100% Utilization*, 1st ed.; Technical Review Company: Tokyo, Japan, 1979; pp. 50–60.